Structure and Dipole Moments of the Two Distinct Solvated Forms of *p*-Nitroaniline in Acetonitrile/CCl_4 As Studied by Infrared Electroabsorption Spectroscopy

Shinsuke Shigeto, Hirotsugu Hiramatsu,† and Hiro-o Hamaguchi*

Department of Chemistry, School of Science, The University of Tokyo, 7-3-1 Hongo, Bunkyo-ku, Tokyo 113-0033, Japan

Received: September 8, 2005; In Final Form: December 3, 2005

Structure and dipole moments of the two distinct solvated forms of *p*-nitroaniline (pNA) in acetonitrile/CCl_4 have been studied by infrared electroabsorption spectroscopy. We measured a series of infrared electroabsorption spectra of pNA dissolved in an acetonitrile/CCl_4 mixed solvent by altering the angle χ between the external electric field and the electric field vector of the incident infrared light. A singular value decomposition analysis has revealed that the observed infrared electroabsorption spectra are decomposed into two major components: the χ-dependent and χ-independent components. The decomposed spectral components as well as the infrared absorption spectrum are well explained in terms of two distinct solvated forms of pNA that exist in equilibrium in the mixed solvent. These solvated forms can be assigned to the 1:1 and 1:2 species, which have one and two acetonitrile molecule(s), respectively, associated with pNA. From a least-squares fitting analysis of the χ-dependent spectral component, it is shown that, for both the 1:1 and 1:2 species, a head-to-tail structure accounts well for the experimental results. On the other hand, the χ-independent component is likely to arise from the population change between the two solvated forms. This electric-field-induced population change of solvated forms may lead to the control of dielectric environments in solution by an external electric field.

Introduction

Solvation is one of the most fundamental phenomena that take place in the solution phase.[1,2] It is well-known that, in a variety of solution-phase chemical processes, solvation plays crucial roles in determining the direction and rate of reactions and in changing the energies of excited as well as the ground states. The solvation in aqueous solutions,[3] which is often termed hydration, is highly important for the structure formation and stability of biomolecules. Solvation has thus been arousing broad and keen interest in various fields of physical chemistry for many years. Owing to recent progresses in ultrashort pulsed lasers, ultrafast solvation dynamics in the femtosecond to picosecond time region has become experimentally accessible.[1−8] Maroncelli and co-workers[1,2,7,8] studied the solvation of dye probe molecules such as coumarin 153 in polar liquids and discussed the solvent reorientation around the photoexcited solute molecule, in terms of the spectral response function derived from a peak shift of time-resolved emission spectra (dynamic Stokes shift). A number of theoretical approaches have also been developed. The dielectric continuum model[9−12] has often been used in the study of solvent effects and solvation dynamics. The integral equation theory for the reference interaction site model (RISM) was developed[13] and extended by taking into account the charge distribution in a molecule, to facilitate applications to more realistic molecular liquids.[14,15] Molecular dynamics simulations[2,16,17] have emerged as a powerful tool for investigating the dynamics involved in solvation, though their application is greatly dependent on the ability of computers available. Despite accumulated information on dynamical aspects of solvation in these extensive studies, direct quantitative information on solvated forms regarding their geometric structures is still scant. Such structural information is not obtainable from relaxation time constants derived from emission spectra. Vibrational spectroscopy is undoubtedly more suitable for the experimental elucidation of solvated structures. It does not need fluorescent probe and hence looks at the system without any external perturbation.

In our previous papers,[18−20] we reported a comprehensive study of the solvation of *p*-nitroaniline (pNA) in acetonitrile (AN)/CCl_4 mixed solvents. pNA is one of the simplest molecules having electron donor and acceptor moieties connected by an aromatic ring. It exhibits pronounced solvatochromism[21,22] and large nonlinear optical properties.[23,24] These and other photochemical features of pNA have long been the subject of various investigations.[25−31] We measured UV absorption and Raman spectra of pNA dissolved in the mixed solvents for different molar fractions of AN, and analyzed them using singular value decomposition (SVD).[19] Interestingly, the result indicated that the observed spectral changes were attributable not to the continuous change of the charge-transfer character of pNA but to the equilibrium change among the free pNA and two distinct solvated forms. By examining the Raman spectra, we were able to assign these forms to the 1:1 species (pNA associated with one AN molecule on the amino group, Figure 1), and the 1:2 species (pNA associated with one AN molecule on the amino group and one on the nitro group, Figure 1).[18,19] Although these qualitative association forms have been determined, quantitative information on the geometric structures of the 1:1 and 1:2 species is yet to be obtained.

In the present study, we try to shed more light on this issue by means of infrared electroabsorption spectroscopy.[32−35] Infrared electroabsorption spectroscopy is able to detect mo-

* Corresponding author. E-mail: hhama@chem.s.u-tokyo.ac.jp.
† Present address: Graduate School of Pharmaceutical Sciences, Tohoku University, Sendai 980-8578, Japan.

10.1021/jp055082y CCC: $33.50
Published on Web 02/17/2006

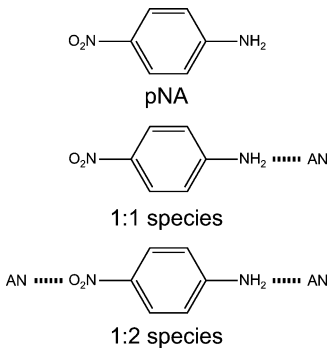

Figure 1. Chemical structure of pNA and proposed structures of two distinct solvated forms of pNA (the 1:1 and 1:2 species).

lecular responses to an external electric field as changes in infrared absorption intensities. Its high sensitivity to molecular structure and feasibility to determine permanent dipole moments have already been demonstrated in the studies of the trans−gauche isomerization of 1,2-dichloroethane,[33] the self-association of *N*-methylacetamide,[34] and association forms of liquid crystal molecules.[35] Because the two solvated forms of pNA would have different permanent dipole moments, they are expected to respond to an applied electric field in a different way through the orientational polarization. It would thus be possible to determine separately the permanent dipole moments of the coexisting solvated forms and hence obtain structural information on these forms, by analyzing the orientational polarization signal. To that end, we measured the angle χ dependence of the infrared electroabsorption spectrum of pNA dissolved in an AN/CCl_4 mixed solvent, where χ is the angle between the applied electric field and the electric field vector of the incident infrared light. We extracted the χ-dependent orientational polarization signal from the infrared electroabsorption spectra using an SVD analysis. Probable structures of the two solvated forms were derived with the aid of ab initio molecular orbital (MO) calculations. The χ-independent spectral component, which we assign to the population change between the 1:1 and 1:2 species, is also discussed in relation to possible manipulation of chemical equilibrium in solution by applying an external electric field.

Theoretical Background

The absorbance change ΔA in electroabsorption measurements arises from several different molecular responses to an applied electric field. In this section, we consider three types of signals that contribute to an infrared electroabsorption spectrum. Some of them prove to be of significance and are examined in the analysis described later.

Orientational Polarization. The most prominent contribution to ΔA in the present experiment is the orientational polarization signal. When an external electric field is applied to a sample, reorientation of polar molecules having the permanent dipole moment μ_P takes place. The orientational anisotropy induced in the sample gives rise to the absorbance change. The absorbance change ratio $\Delta A/A$ is given by[32]

$$\frac{\Delta A}{A} = \frac{1}{12}\left(\frac{\mu_P F}{k_B T}\right)^2 (1 - 3\cos^2\eta)(1 - 3\cos^2\chi) \qquad (1)$$

Here η is the angle between μ_P and the transition dipole moment μ_T of the vibrational mode of interest, F is the internal (local-field-corrected) electric field, k_B is the Boltzmann constant, and T is the temperature. Equation 1 holds under the condition $\mu_P F \ll k_B T$, which is satisfied in the present study ($\mu_P F/k_B T < 0.1$). Once the $\Delta A/A$ value due to the orientational polarization is obtained from the χ-dependence measurement of an infrared electroabsorption spectrum, we can derive structural information on the molecule through parameters μ_P and η on the basis of eq 1.

Electronic Polarization. The absorbance change also originates from the change in electronic properties of a molecule caused by the applied electric field. Assuming that the orientational distribution of molecules is uniform and the terms up to the second order in F are retained, the electronic polarization signal $\Delta A(\tilde{\nu})$ can be written in the form[36,37]

$$\Delta A(\tilde{\nu}) = F^2\left[A_\chi A(\tilde{\nu}) + \frac{B_\chi}{15hc}\tilde{\nu}\frac{d}{d\tilde{\nu}}\frac{A(\tilde{\nu})}{\tilde{\nu}} + \frac{C_\chi}{30h^2c^2}\tilde{\nu}\frac{d^2}{d\tilde{\nu}^2}\frac{A(\tilde{\nu})}{\tilde{\nu}}\right] \qquad (2)$$

where $\tilde{\nu}$ is the wavenumber, c is the speed of light, and h is Planck's constant. The coefficients A_χ, B_χ, and C_χ are intimately related to molecular properties of the sample such as μ_T, the transition polarizability, and the transition hyperpolarizability.[37] It can be seen from eq 2 that the electronic polarization signal is expressed by the zeroth, first, and second derivatives of the absorption band $A(\tilde{\nu})$. As was estimated by MO calculations under applied electric fields,[32] the zeroth-derivative term (A_χ term) is considerably small compared with the present detection limit, even if we apply the electric field whose magnitude is 10^2 times as large as that currently used in our experiment. We can thus disregard the contribution of the electronic polarization signal to the zeroth-derivative term.

Population Change. Besides the above-mentioned two signals, the equilibrium change caused by an external electric field may be observed in some cases. If the stabilization due to the dipole interaction with the applied electric field differs among coexisting molecular species in solution, the equilibrium shifts toward more stabilized species. A good example that gives the population change signal is the trans−gauche isomerism of 1,2-dichloroethane, which has been analyzed in detail previously.[33] As will be discussed in the subsequent section, the population change signal is also observed for pNA in AN/CCl_4 mixed solvents.

Experiments and Analyses

The experimental apparatus and the sample cell used for infrared electroabsorption spectroscopy have been described elsewhere.[32] The main characteristic of this setup is the use of a dispersive infrared spectrometer and an AC-coupled amplifier, which enables one to detect minute absorbance change ΔA as small as 6×10^{-8}.[32] A 25 kHz sinusoidal wave of an electric field whose amplitude was 1.5×10^7 V m^{-1} was applied across the cell gap of about 5 μm. The intensity change of the transmitted infrared light with 50 kHz modulation, twice the frequency of the applied electric field, was detected with a lock-in amplifier. Infrared absorption spectra were also measured with a KBr sample cell with a 100 μm spacer. When the angle χ dependence of the infrared electroabsorption spectrum was measured, the incident infrared light was p-polarized with respect to the cell window.

All the reagents (*p*-nitroaniline, HPLC-grade dehydrated acetonitrile and carbon tetrachloride) were commercially obtained and used as received. pNA was dissolved in a mixed solvent of AN (10 vol %) and CCl_4 (90 vol %) whose molar fraction of AN was 0.17. The concentration of pNA was 0.03 mol dm^{-3}. All measurements were conducted at room temper-

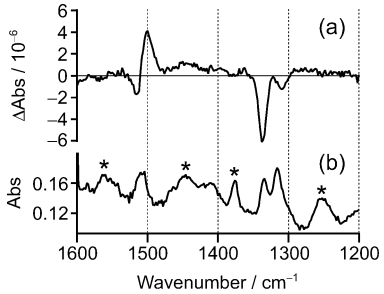

Figure 2. Infrared electroabsorption spectrum (a) and infrared absorption spectrum (b) of pNA in the AN/CCl_4 mixed solvent. The infrared electroabsorption spectrum was measured with the normal incidence of the infrared light. Asterisks represent the solvent bands.

ature. We used Igor Pro 5 (WaveMetrics, Inc.) for performing SVD and least-squares fittings and the *Gaussian 98* program[38] for MO calculations.

Results and Discussion

Infrared Electroabsorption Spectrum. Figure 2 shows a typical infrared electroabsorption spectrum (ΔA spectrum, Figure 2a) and infrared absorption spectrum (Figure 2b) of pNA in the AN/CCl_4 mixed solvent in the wavenumber region 1600−1200 cm^{-1}. The ΔA spectrum was measured with the normal incidence of the infrared light. Two features in the 1530−1480 and 1360−1300 cm^{-1} regions are clearly observed in the ΔA spectrum. These are assigned to the NO_2 antisymmetric and symmetric stretch modes of pNA, respectively. Note that solvent bands indicated by asterisks in Figure 2b do not appear in the ΔA spectrum. The absorption bands at around 1560 and 1250 cm^{-1} are assigned to CCl_4. It is not surprising that no corresponding peaks are observed in the ΔA spectrum, because CCl_4 does not have a dipole moment that causes orientational polarization. However, the absence of the acetonitrile bands (∼1450 and 1378 cm^{-1}) in the ΔA spectrum is rather unexpected, because the permanent dipole moment[39] of acetonitrile (∼4 D) is not so small compared with that of pNA (∼6 D). This result is indicative of the local structure formation of AN molecules that makes the effective dipole moment small or even zero. The doublet observed in the NO_2 symmetric stretch region corresponds to the contribution of the 1:1 (∼1336 cm^{-1}) and 1:2 (∼1315 cm^{-1}) species.[19] Free pNA gives the NO_2 symmetric stretch band at 1338 cm^{-1}.[19] As will be shown later, its contribution is estimated to be small in the present experiment. Concerning the assignment of the doublet, several authors[29,30] argued that it can be attributed to a Fermi resonance between the NO_2 symmetric stretch band and the combination band of the 491 and 842 cm^{-1} out-of-plane deformation modes. However, the present result as well as the previous SVD analysis[19] and time-resolved visible absorption study[20] confirm our interpretation that pNA forms specific solvated structures in AN. In the ΔA spectrum, the two solvated forms of pNA appear in a very different manner. This result is an unequivocal manifestation of the fact that extra information is available in infrared electroabsorption spectroscopy compared with ordinary infrared absorption. To extract the orientational polarization signal from the ΔA spectrum and obtain direct structural information, the χ dependence of the ΔA spectrum needs to be measured. We focus on the NO_2 symmetric stretch mode in the following χ-dependence measurement and analysis. The NO_2 antisymmetric stretch mode does not show clearly separated bands corresponding to the 1:1 and 1:2 species, making the analysis less meaningful than that for the symmetric stretch.

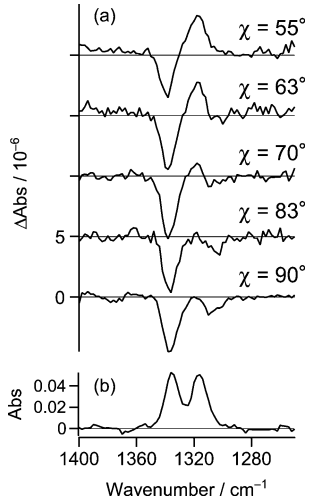

Figure 3. Angle χ dependence of infrared electroabsorption spectrum (a) and solvent-subtracted infrared absorption spectrum (b) of pNA in the AN/CCl_4 mixed solvent.

χ Dependence of Infrared Electroabsorption Spectrum. We measured the ΔA spectra by altering the angle χ from 55° to 90° (normal incidence). The result is shown in Figure 3a, together with the solvent-subtracted absorption spectrum in Figure 3b. The path-length difference due to the rotation of the sample cell and the refraction at the interfaces between the sample and the cell windows has been corrected in each spectrum by using the refractive index of the mixed solvent. The χ-dependent ΔA spectra in Figure 3a exhibit complicated behavior, so that some mathematical posttreatment is required for finding out independent spectral components that have different χ dependences. Here we use an SVD analysis,[19,40−43] which has already found many successful applications, particularly in time-resolved vibrational spectroscopy.[40]

SVD is a mathematical procedure that decomposes an arbitrary matrix **A** with m rows and n columns ($m \times n$, $m > n$) into three matrices **U**, **W**, and **V** as

$$\mathbf{A} = \mathbf{U}\mathbf{W}\mathbf{V}^{\mathrm{T}} \tag{3}$$

where **U**, **W**, and **V** represent a real column-orthogonal matrix ($m \times n$), a real diagonal matrix ($n \times n$), and a real orthogonal matrix ($n \times n$), respectively. The diagonal elements of **W** are called singular values. In the present case, the observed set of the χ-dependent ΔA spectra constitutes the matrix **A**, and each column of the matrices **U** and **V** corresponds to the χ dependence and the intrinsic spectrum, respectively. Usefulness of SVD lies in the fact that we can concentrate only on the spectral components with singular values meaningfully larger than the others and can neglect the remaining singular values as noises. Figure 4 plots the singular values obtained from SVD of the set of the ΔA spectra shown in Figure 3a. Obviously, there are two principal singular values, indicating that the observed set of the ΔA spectra can be well reproduced by considering only two sorts of χ dependence, that is, the χ-independent (constant) component and the χ-dependent component that varies according to the function $1 - 3\cos^2\chi$ (see eq 1). In this case, eq 3 can be reduced as

$$\mathbf{A} \approx (\mathbf{u}_1 \ \ \mathbf{u}_2)\begin{pmatrix} w_1 & 0 \\ 0 & w_2 \end{pmatrix}\begin{pmatrix} \mathbf{v}_1 \\ \mathbf{v}_2 \end{pmatrix} \tag{4}$$

Here vectors **u** and **v** correspond to the χ dependence and the intrinsic spectra accompanied by the largest two singular values

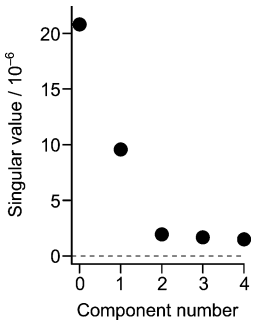

Figure 4. Singular values obtained from the SVD analysis of the χ dependence of infrared electroabsorption spectrum of pNA in the AN/CCl_4 mixed solvent.

w_1 and w_2, respectively. Because SVD is a purely mathematical procedure involving no physical constraint, vectors **u** and **v** do not have physical meanings as they are. However, by taking a proper linear combination (represented by a 2×2 transformation matrix **K**) of these vectors based on the model for the χ dependence, we can have physically meaningful vectors **u**′ and **v**′:

$$\mathbf{A} \approx (\mathbf{u}_1 \ \ \mathbf{u}_2)\mathbf{K}^{-1}\mathbf{K}\begin{pmatrix} w_1 & 0 \\ 0 & w_2 \end{pmatrix}\begin{pmatrix} \mathbf{v}_1 \\ \mathbf{v}_2 \end{pmatrix} = (\mathbf{u}'_1 \ \ \mathbf{u}'_2)\begin{pmatrix} \mathbf{v}'_1 \\ \mathbf{v}'_2 \end{pmatrix} \quad (5)$$

with

$$(\mathbf{u}'_1 \ \ \mathbf{u}'_2) = (\mathbf{u}_1 \ \ \mathbf{u}_2)\mathbf{K}^{-1} \quad (6)$$

$$\begin{pmatrix} \mathbf{v}'_1 \\ \mathbf{v}'_2 \end{pmatrix} = \mathbf{K}\begin{pmatrix} w_1 & 0 \\ 0 & w_2 \end{pmatrix}\begin{pmatrix} \mathbf{v}_1 \\ \mathbf{v}_2 \end{pmatrix} \quad (7)$$

In the present study, the transformation matrix **K** has been determined by least-squares fittings so that the theoretically expected dependence, namely, the constant and the $1 - 3\cos^2 \chi$ dependence, is reproduced. The χ dependence obtained ($\mathbf{u}'_1$ and $\mathbf{u}'_2$) as well as the expected dependence are shown in Figure 5a. The corresponding spectral components ($\mathbf{v}'_1$ and $\mathbf{v}'_2$) are shown in Figure 5b. In Figure 6, the ΔA spectra reconstructed according to eq 5 are compared with the observed ΔA spectra. The entire agreement between the observed and reconstructed spectra ensures that the above SVD analysis is correct. Hereafter, we discuss the solvated structures of pNA on the basis of these decomposed spectral components.

χ-Dependent Component. First, we examine the χ-dependent spectral component. We carried out a least-squares fitting analysis for both the infrared absorption spectrum and the χ-dependent ΔA spectrum, assuming the contributions of the 1:1 and 1:2 species. The contribution of the free species is neglected to reduce the number of adjustable parameters in the fitting analysis. Note that the abundance ratio of the free, 1:1, and 1:2 species of pNA determined in our previous study[19] was about 1:3:4 at the AN molar fraction of 0.17. The infrared absorption spectrum was first fitted with Lorentzian line shapes to obtain the peak positions and the bandwidths. These values were then fixed and used for fitting the χ-dependent ΔA spectrum, in which we included the zeroth and first derivatives of the absorption band for the 1:1 species and the zeroth derivative for the 1:2 species. The fitting result is shown in Figure 7. Both the infrared absorption spectrum and the χ-dependent spectral component of the infrared electroabsorption spectra are fitted very well. Because the contribution of the electronic polarization signal to the zeroth-derivative component is generally too small to be detected in our experiment,[32] the

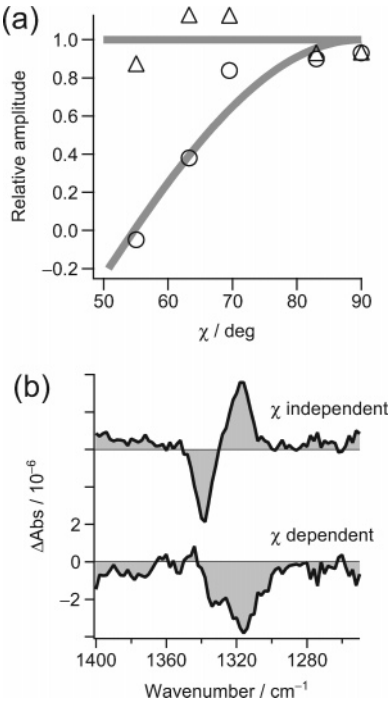

Figure 5. Results of the SVD analysis of the χ-dependent infrared electroabsorption spectra of pNA in the AN/CCl_4 mixed solvent. (a) Observed χ dependence (circles and triangles) and model functions (thick lines). (b) χ-Independent and χ-dependent spectral components.

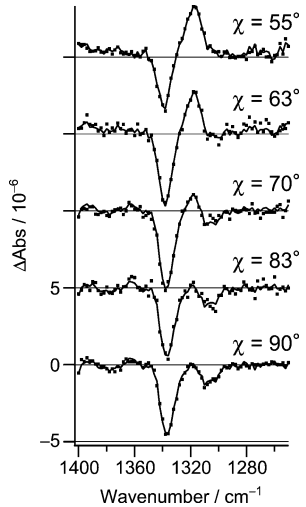

Figure 6. Observed (dots) and reconstructed (solid lines) χ-dependent infrared electroabsorption spectra of pNA in the AN/CCl_4 mixed solvent.

zeroth-derivative components for both the 1:1 and 1:2 species are thought to originate from the orientational polarization signal. In contrast, the necessity for including the first-derivative component for the 1:1 species may indicate that the electronic polarization signal does contribute to the infrared electroabsorption spectra through the first- and perhaps second-derivative terms.

The experimental absorbance change ratio $\Delta A/A$ for the orientational polarization signal can be calculated from the amplitude of the zeroth-derivative component of the ΔA spectrum and the absorbance A of the infrared absorption spectrum. The $\Delta A/A$ values of the 1:1 and 1:2 species are listed in Table 1. The $\Delta A/A$ value of the 1:2 species is about 3 times as large as that of the 1:1 species. It is not until the χ-dependent spectral component has been derived from the SVD analysis that accurate $\Delta A/A$ values, which directly connect the experi-

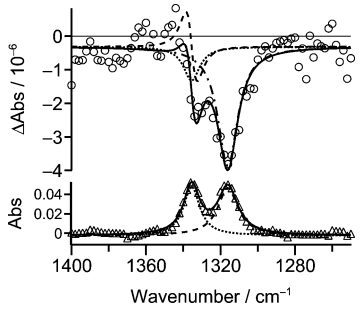

Figure 7. Results of the fitting analysis of the χ-dependent spectral component and infrared absorption spectrum of pNA in the AN/CCl_4 mixed solvent. Upper: decomposition of the χ-dependent spectral component: circles, observed χ-dependent spectrum; solid line, fitted curve; dotted line, zeroth derivative of the infrared absorption band of the 1:1 species; dashed line, first derivative of the infrared absorption band of the 1:1 species; dotted dashed line, zeroth derivative of the infrared absorption band of the 1:2 species. Lower: decomposition of the infrared absorption spectrum of pNA in the AN/CCl_4 mixed solvent: triangles, observed infrared absorption spectrum; solid line, fitted curve; dotted line, contribution of the 1:1 species; dashed line, contribution of the 1:2 species.

TABLE 1: Observed and Calculated $\Delta A/A$ Values for Orientational Polarization Signal

	1:1 species	1:2 species
observed $\Delta A/A$	$-(5 \pm 1) \times 10^{-4}$	$-(18 \pm 4) \times 10^{-4}$
calculated $\Delta A/A$	-8×10^{-4}	-13×10^{-4}

mental results with geometric structures of the solvated forms, are determined.

At this point, we are able to discuss possible solvated structures of the 1:1 and 1:2 species. We performed ab initio MO calculations at the HF/6-31+G** level using the *Gaussian 98* program[38] for both the 1:1 and 1:2 species. Starting from several initial geometries, two head-to-tail-like optimized structures were obtained for these species. They are shown in Figure 8. The obtained structural parameters μ_P and η are 11 D and 155° for the 1:1 species, and 16 D and 149° for the 1:2 species, respectively. Note that η is the angle between μ_P and μ_T of the NO_2 symmetric stretch mode. The values of the permanent dipole moment of both the 1:1 and 1:2 species compare favorably with those expected from the literature values[39] for pNA (~6 D) and AN (~4 D). The calculated frequencies of the NO_2 symmetric stretch mode in free pNA, the 1:1 species, and the 1:2 species are 1606, 1597, and 1586 cm^{-1}, respectively. If we scale these frequencies so that the calculated frequency of the free species agrees with the observed, the other calculated frequencies become 1330 and 1321 cm^{-1}. Those scaled frequencies are in good accordance with the observed frequencies, 1336 and 1315 cm^{-1}. Substituting the μ_P and η values into eq 1, we can calculate the $\Delta A/A$ value on the basis of the model structures derived from the MO calculations. The calculated $\Delta A/A$ values are shown in Table 1. Here we have set the internal electric field F to be 0.6 times as large as the external electric field (1.5×10^7 V m^{-1}) by using acetone/CCl_4 solution as a standard.[32] We suppose the main cause of this amplitude decrease is the voltage drop at the electrode. The permanent dipole moments obtained from the MO calculations are the values in a vacuum; therefore, they are estimated to be somewhat larger than those in solution. Taking this fact into consideration, the calculated $\Delta A/A$ values are in good agreement with the observed values. In other words, head-to-tail structures similar to the structures shown in Figure 8 are probable structures for both the 1:1 and 1:2 species. Another possible structure, an antiparallel structure, gives the $\Delta A/A$ value of $\sim 0.8 \times 10^{-4}$ for the 1:1 species, which does not account for the experimentally determined $\Delta A/A$ value at all. It should be noted that such an experimental determination of each solvated structure in solution is hardly done with other experimental method but infrared electroabsorption spectroscopy.

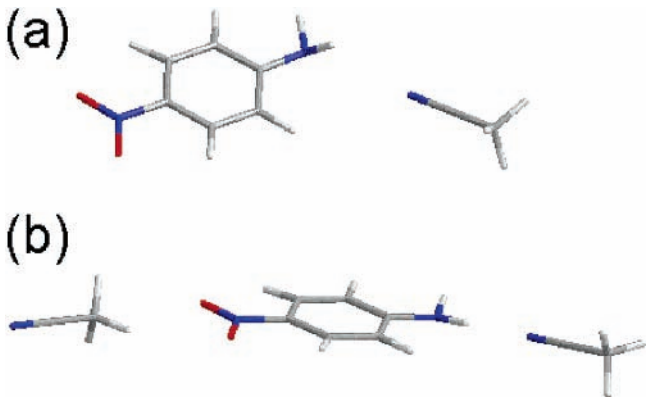

Figure 8. Optimized structures of the 1:1 species (a) and the 1:2 species (b) obtained from ab initio MO calculation (HF/6-31+G** level).

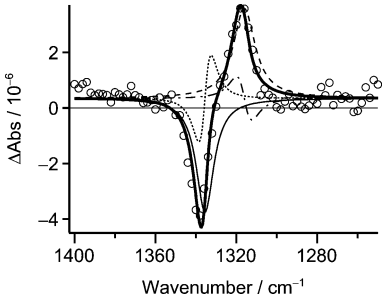

Figure 9. Results of the fitting analysis of the χ-independent spectral component: circles, observed χ-independent spectrum; thick solid line, fitted curve; thin solid line, zeroth derivative of the infrared absorption band of the 1:1 species; dotted line, first derivative of the infrared absorption band of the 1:1 species; dashed line, zeroth derivative of the infrared absorption band of the 1:2 species; dotted dashed line, first derivative of the infrared absorption band of the 1:2 species.

χ-Independent Component. The χ-independent component is also examined by the same fitting analysis. In this case, the first derivative of the absorption band is additionally incorporated for the 1:2 species for a better fit. Shown in Figure 9 is the fitting result. The first-derivative components of both the 1:1 and 1:2 species are again ascribable to the electronic polarization signal. Then what is the origin of the zeroth-derivative components? It is not likely that the electronic polarization is responsible for the zeroth-derivative component for the same reason invoked in the analysis of the χ-dependent component. The most plausible reason for the origin of the zeroth-derivative components of the χ-independent spectrum is, at present, the population change between the 1:1 and 1:2 species. The two solvated species exist in equilibrium in the mixed solvent:[19] pNA (1:1) + AN $\rightleftharpoons$ pNA (1:2). As we have determined in the previous subsection, the 1:2 species has a larger permanent dipole moment than the 1:1 species. Therefore, the 1:2 species would be more stabilized than the 1:1 species via the dipole interaction with the applied electric field, which results in an increase (positive zeroth-derivative signal) of the 1:2 species and a concomitant decrease (negative zeroth-derivative signal) of the 1:1 species. This expectation on the sign of the zeroth-derivative signals for the 1:1 and 1:2 species accords well with the experimental result (see the thin solid line and dashed line in Figure 9). The $\Delta A/A$ values of the 1:1 and 1:2 species determined by the fitting are -2×10^{-4} and

$+2 \times 10^{-4}$, respectively. It can thus be concluded that ~0.02% of the 1:1 species undergo further solvation of an acetonitrile molecule and generate the 1:2 species. This result formally indicates that the distribution of solvated forms in solution could be changed with an applied electric field. It may offer possibilities for switching solvated structures to start and/or promote a particular chemical reaction by an external electric field. In this context, infrared electroabsorption spectroscopy will also provide important and otherwise unobtainable information on electric properties of molecules in liquids/solutions.

Conclusions

In this paper, we have studied the solvated structures of pNA dissolved in the AN/CCl_4 mixed solvent with infrared electroabsorption spectroscopy. The χ dependence of the infrared electroabsorption spectrum of pNA in the NO_2 symmetric stretch region (1400−1250 cm^{-1}) has been analyzed in detail by employing SVD. The SVD analysis has revealed that the observed infrared electroabsorption spectra are decomposed into two dominant components that show the $1 - 3\cos^2\chi$ and constant χ dependence. From the fitting analysis of the χ-dependent spectral component in conjunction with ab initio MO calculations, it is shown that a head-to-tail structure is most probable for both the 1:1 and 1:2 species. Such quantitative insight into the geometric structures of the two distinct solvated forms of pNA has been gained for the first time. We have also examined the χ-independent spectral component. The zeroth-derivative signal of the χ-independent component is attributed to the population change between the two distinct solvated forms due to the applied electric field. The trend found in the zeroth-derivative signals of the 1:1 and 1:2 species is consistent with that predicted from the probable structures of these species. We believe that infrared electroabsorption spectroscopy can provide a new basis for elucidating electric properties and structures of molecules associated with solvation and hence opening up new possibilities for controlling dielectric environment in liquids/solutions.

References and Notes

(1) Stratt, R. M.; Maroncelli, M. *J. Phys. Chem.* **1996**, *100*, 12981.
(2) Maroncelli, M. *J. Mol. Liq.* **1993**, *57*, 1.
(3) Nandi, N.; Bhattacharyya, K.; Bagchi, B. *Chem. Rev.* **2000**, *100*, 2013.
(4) Barbara, P. F.; Jarzeba, W. *Adv. Photochem.* **1990**, *15*, 1.
(5) de Boeij, W. P.; Pshenichnikov M. S.; Wiersma D. A. *Annu. Rev. Phys. Chem.* **1998**, *49*, 99.
(6) Berg, M.; Vanden Bout, D. A. *Acc. Chem. Res.* **1997**, *30*, 65.
(7) Castner, E. W., Jr.; Maroncelli, M.; Fleming, G. R. *J. Chem. Phys.* **1987**, *86*, 1090.
(8) Maroncelli, M.; Fleming G. R. *J. Chem. Phys.* **1987**, *86*, 6221.
(9) Born, M. *Z. Phys.* **1920**, *1*, 45.
(10) Onsager, L. *J. Am. Chem. Soc.* **1936**, *58*, 1486.
(11) Marcus, R. A. *J. Chem. Phys.* **1956**, *24*, 966. Marcus, R. A. *J. Chem. Phys.* **1956**, *24*, 979.
(12) Bagchi, B. *Annu. Rev. Phys. Chem.* **1989**, *40*, 115.
(13) Chandler, D.; Anderson, H. C. *J. Chem. Phys.* **1972**, *57*, 1930.
(14) Hirata, F.; Rossky, P. J. *Chem. Phys. Lett.* **1981**, *83*, 329.
(15) Hirata, F. *Bull. Chem. Soc. Jpn.* **1998**, *71*, 1483.
(16) Maroncelli, M.; Kumar, V. P.; Papazyan, A. *J. Phys. Chem.* **1993**, *97*, 13.
(17) Fonseca, T.; Ladanyi, B. M. *J. Mol. Liq.* **1994**, *60*, 1.
(18) Mohanalingam, K.; Hamaguchi, H. *Chem. Lett.* **1997**, 157.
(19) Mohanalingam, K.; Yokoyama, D.; Kato, C.; Hamaguchi, H. *Bull. Chem. Soc. Jpn.* **1999**, *72*, 389.
(20) Mohanalingam, K.; Yamaguchi, S.; Hamaguchi, H. *Laser Chem.* **1999**, *19*, 329.
(21) Khalil, O. S.; Seliskar, C. J.; McGlynn, S. P. *J. Chem. Phys.* **1973**, *58*, 1607.
(22) Carsey, T. P.; Findley, G. L.; McGlynn, S. P. *J. Am. Chem. Soc.* **1979**, *101*, 4502.
(23) Karna, S. P.; Prasad, P. N.; Dupuis, M. *J. Chem. Phys.* **1991**, *94*, 1171.
(24) Woodford, J. N.; Pauley, M. A.; Wang, C. H. *J. Phys. Chem. A* **1997**, *101*, 1989.
(25) Sinha, H. K.; Yates, K. *Can. J. Chem.* **1991**, *69*, 550.
(26) Schuddeboom, W.; Warman, J. M.; Biemans, H. A. M.; Meijer, E. W. *J. Phys. Chem.* **1996**, *100*, 12369.
(27) Thomsen, C. L.; Thøgersen, J.; Keiding, S. R. *J. Phys. Chem. A* **1998**, *102*, 1062.
(28) Kovalenko, S. A.; Schanz, R.; Farztdinov, V. M.; Hennig, H.; Ernsting, N. P. *Chem. Phys. Lett.* **2000**, *323*, 312.
(29) Moran, A. M.; Kelley, A. M. *J. Chem. Phys.* **2001**, *115*, 912.
(30) Kozich, V.; Werncke, W.; Dreyer, J.; Brzezinka, K.-W.; Rini, M.; Kummrow, A.; Elsaesser, T. *J. Chem. Phys.* **2002**, *117*, 719.
(31) Schrader, T.; Sieg, A.; Koller, F.; Schreier, W.; An, Q.; Zinth, W.; Gilch, P. *Chem. Phys. Lett.* **2004**, *392*, 358.
(32) Hiramatsu, H.; Hamaguchi, H. *Appl. Spectrosc.* **2004**, *58*, 355.
(33) Hiramatsu, H.; Kato, C.; Hamaguchi, H. *Chem. Phys. Lett.* **2001**, *347*, 403.
(34) Hiramatsu, H.; Hamaguchi, H. *Chem. Phys. Lett.* **2002**, *361*, 457.
(35) Min, Y.-K.; Hiramatsu, H.; Hamaguchi, H. *Chem. Lett.* **2002**, 68.
(36) Varma, C. A. G. O.; Oosterhoff, L. J. *Chem. Phys. Lett.* **1971**, *8*, 1.
(37) Andrews, S. S.; Boxer, S. G. *J. Phys. Chem. A* **2000**, *104*, 11853.
(38) Frisch, M. J.; Trucks, G. W.; Schlegel, H. B.; Scuseria, G. E.; Robb, M. A.; Cheeseman, J. R.; Zakrzewski, V. G.; Montgomery, J. A., Jr.; Stratmann, R. E.; Burant, J. C.; Dapprich, S.; Millam, J. M.; Daniels, A. D.; Kudin, K. N.; Strain, M. C.; Farkas, O.; Tomasi, J.; Barone, V.; Cossi, M.; Cammi, R.; Mennucci, B.; Pomelli, C.; Adamo, C.; Clifford, S.; Ochterski, J.; Petersson, G. A.; Ayala, P. Y.; Cui, Q.; Morokuma, K.; Malick, D. K.; Rabuck, A. D.; Raghavachari, K.; Foresman, J. B.; Cioslowski, J.; Ortiz, J. V.; Baboul, A. G.; Stefanov, B. B.; Liu, G.; Liashenko, A.; Piskorz, P.; Komaromi, I.; Gomperts, R.; Martin, R. L.; Fox, D. J.; Keith, T.; Al-Laham, M. A.; Peng, C. Y.; Nanayakkara, A.; Gonzalez, C.; Challacombe, M.; Gill, P. M. W.; Johnson, B. G.; Chen, W.; Wong, M. W.; Andres, J. L.; Head-Gordon, M.; Replogle, E. S.; Pople, J. A. *Gaussian 98*, revision A.9; Gaussian, Inc.: Pittsburgh, PA, 1998.
(39) McClellan, A. L. *Tables of Experimental Dipole Moments*; W. H. Freeman: San Francisco and London, 1963.
(40) Hashimoto, M.; Yuzawa, T.; Kato, C.; Iwata, K.; Hamaguchi, H. In *Handbook of Vibrational Spectroscopy*; Chalmers, J. M., Griffiths, P. R., Eds.; John Wiley & Sons: Chichester, U.K., 2002; Vol. 1, pp 666−676.
(41) Chen, W.-G.; Braiman, M. *Photochem. Photobiol.* **1991**, *54*, 905.
(42) Zimányi, L.; Kulcsár, Á.; Lanyi, J. K.; Sears, D. F., Jr.; Saltiel, J. *Proc. Natl. Acad. Sci. U.S.A.* **1999**, *96*, 4408.
(43) Chung, H. S.; Khalil, M.; Tokmakoff, A. *J. Phys. Chem. B* **2004**, *108*, 15332.